

Electronic Supporting information

**Efficient Thermally Activated Delayed Fluorescent
Emitters Based on Parallel Aligned Bi-spiro-acridine
Donor**

Hao Peng,^{a†} Jingli Lou,^{b†} Ganggang Li,^b Changjiang Zhou,^c Zhiming Wang,^b He Liu^{a}*

^a College of Materials Science and Engineering, Shenzhen University, Shenzhen 518060, P. R. China.

E-mail: liuhe001@szu.edu.cn

^b State Key Laboratory of Luminescent Materials and Devices, Center for Aggregation-Induced Emission, Guangzhou International Campus, South China University of Technology (SCUT), Guangzhou 510640, P. R. China.

^c College of Chemical Engineering, Zhejiang University of Technology, Hangzhou 310014, P. R. China.

† These authors contribute equally to this work

General information

All oxygen- and moisture-sensitive manipulations were carried out under an inert atmosphere. All the chemicals were purchased from commercial sources and used as received unless stated otherwise. Toluene was refluxed over Na and distilled under dry argon. Synthesized compounds were subject to purification by temperature gradient sublimation in high vacuum before used in subsequent studies. The ^1H and ^{13}C NMR spectra were recorded on a Bruker Ascend spectrometer using CDCl_3 as solvent and tetramethylsilane (TMS) as an internal reference. Mass analyses were recorded by Bruker autoflex MALDI-TOF mass spectrometer. UV-Vis absorption spectra were recorded on a Shimadzu UV-2700 recording spectrophotometer. Photoluminescence (PL) spectra were recorded on a Hitachi F-4600 fluorescence spectrophotometer. Phosphorescence spectra of thin films were conducted at 77 K. Thermogravimetric analysis (TGA) was recorded on a TA Q50 instrument under nitrogen atmosphere at a heating rate of $10\text{ }^\circ\text{C}/\text{min}$ from 25 to $800\text{ }^\circ\text{C}$. The temperature of degradation (T_d) was correlated to a 5% weight loss. Differential scanning calorimetry were carried out on a TA Q200. The glass transition temperature (T_g) was determined from the second heating scan at a heating rate of $10\text{ }^\circ\text{C min}^{-1}$ from 25 to $400\text{ }^\circ\text{C}$. Cyclic voltammetry (CV) was carried out in nitrogen-purged tetrahydrofuran or acetonitrile (reduction scan) or dichloromethane (oxidation scan) at room temperature with a CHI voltammetric analyzer. Tetrabutylammonium hexafluorophosphate (0.1 M) was used as the supporting electrolyte. The conventional three-electrode configuration consisted of a platinum working electrode, a platinum wire auxiliary electrode and an Ag wire pseudo-reference electrode with ferrocenium/ferrocene (Fc^+/Fc) as the internal standard. Cyclic voltammograms were obtained at scan rate of 100 mV/s . Formal potentials were calculated as the average of cyclic voltammetric anodic and cathodic peaks. The HOMO energy levels of the compounds were calculated according to the formula: $-[4.8 + (E_{1/2(\text{ox/red})} - E_{1/2(\text{Fc/Fc}^+)})]\text{ eV}$. The onset potential was determined from the intersection of two tangents drawn at the rising and background current of the cyclic voltammogram. The PL lifetimes were measured by a single photon counting spectrometer from Edinburgh Instruments (FLS920) with a Picosecond Pulsed UV-

LASTER (LASTER377) as the excitation source. The solid state absolute PLQYs were measured on a Hamamatsu UV-NIR absolute PL quantum yield spectrometer (C13534, Hamamatsu Photonics) equipped with a calibrated integrating sphere in the host of DPEPO (10 wt%) under excitation of 300 nm. During the PLQY measurements, the integrating sphere was purged with pure and dry argon to maintain an inert environment. The ground state molecular structures were optimized at the B3LYP-D3/6-31g** level of theory; the S_1 and T_1 geometries were optimized *via* time-dependent DFT (TDDFT) at PBE0/def2-SVP level of theory. In addition, the overlaps between the hole and electron density distributions in the S_1 and T_1 states were estimated by the Multiwfn code.^[1]

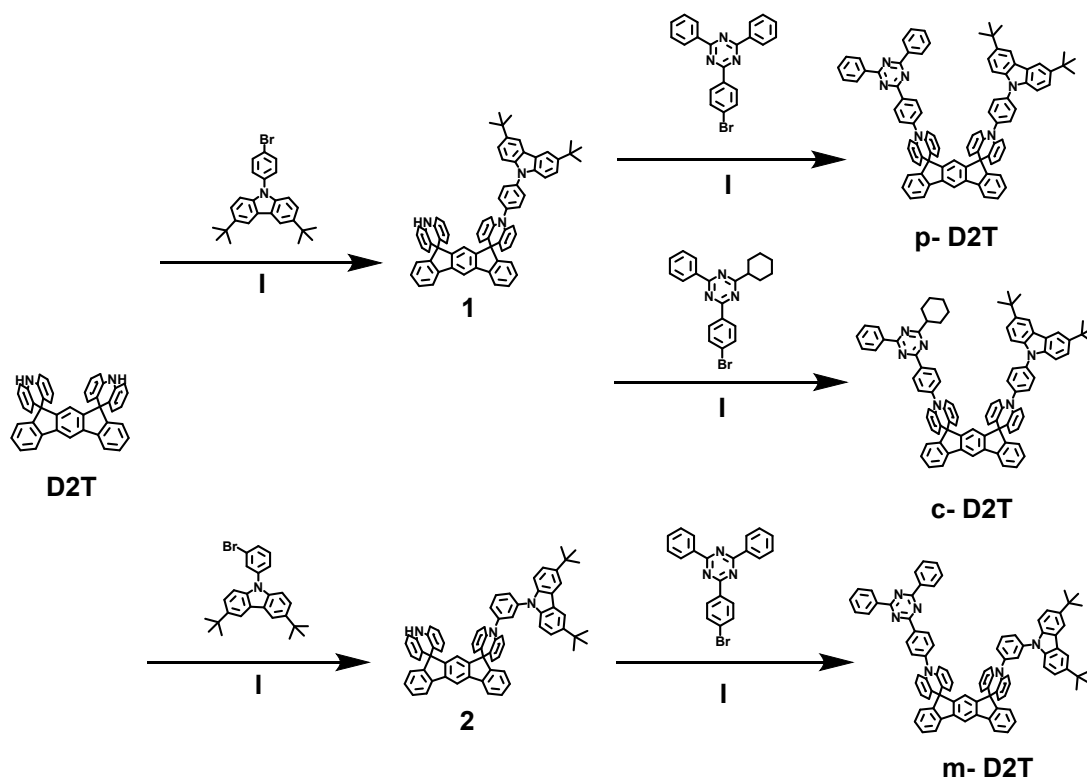
Device Fabrication

Glass substrates pre-coated with a 95-nm-thin layer of indium tin oxide (ITO) with a sheet resistance of 20 Ω per square were thoroughly cleaned for 10 minutes in ultrasonic bath of acetone, isopropyl alcohol, detergent, deionized water, and isopropyl alcohol. Then, the substrates were totally dried in a 75 °C oven. After that, in order to improving the hole injection ability of ITO, the substrates were treated by O_2 plasma for 10 minutes. Multilayer OLEDs were fabricated by the vacuum-deposition method. Organic layers were deposited by high-vacuum ($\sim 5 \times 10^{-4}$ Pa) thermal evaporation onto a glass substrate pre-coated with an ITO layer. All organic layers were deposited sequentially. The thermal deposition rates for the organic materials, LiF and Al were 1.0~1.5, 0.1 and 3~5 \AA s^{-1} , respectively. The active area of each device was 9 mm². The electroluminescence spectra, the current density-voltage characteristics and the current density-voltage-luminance curves characterizations of the OLEDs were carried out with a Photo Research SpectraScan PR-745 Spectroradiometer and a Keithley 2450 Source Meter and they are recorded simultaneously. All measurements were done at room temperature under ambient conditions.

Synthesis

m-dibromobenzene, 1-bromo-4-iodobenzene, 3,6-di-*tert*-butylcarbazole, cesium

carbonate, cuprous iodide, palladium (0) tetrakis(triphenylphosphine), potassium carbonate, 1,10-anhydrous phenanthroline, were used as received. 9-(4-bromophenyl)-3,6-di-tert-butyl-9H-carbazole and 9-(3-bromophenyl)-3,6-di-tert-butyl-9H-carbazole was synthesized according to reference.^[2] 2-chloro-4-cyclohexyl-6-phenyl-1,3,5-triazine was synthesized according to reference.^[3] D2T was synthesized according to reference.^[4]



I: Pd(OAc)₂, *t*-BuONa, *t*-Bu₃PHBF₄, toluene, 110 °C, 12 h.

Scheme S1. Synthetic route of p-D2T, m-D2T and c-D2T.

Synthesis of *10-(4-(3,6-di-tert-butyl-9H-carbazol-9-yl)phenyl)-10H,10''H-dispiro[acridine-9,10'-indeno[2,1-b]fluorene-12',9''-acridine](1)*

D2T (1 g, 1.72 mmol) and 9-(4-bromophenyl)-3,6-di-tert-butyl-9H-carbazole (624 mg, 1.44 mmol) and toluene (50 mL) were added into a 250 mL double neck flask in N₂ atmosphere. The mixture was degassed for 10 min, acetic acid palladium (II) (73 mg, 0.325 mmol), sodium tert-butoxide (277 mg, 2.88 mmol), and tri-tert-butylphosphine tetrafluoroborate (189 mg, 0.65 mmol) were added. The mixture was heated to 110 °C and continually stirred for 8 h. After cooling and vacuum filtrating,

the filtrate was evaporated under reduced pressure. Purification via column chromatography on silica gel (300-400 mesh, petroleum ether/dichloromethane = 2:1, v/v) afforded a as a white solid (0.8 g, 60% yield). ¹H NMR (400 MHz, CDCl₃): δ (ppm) 8.27 (s, 1H, Ar-H), 8.18 (s, 2H, Ar-H), 7.91-7.85 (m, 4H, Ar-H), 7.63-7.61 (d, *J* = 8 Hz, 2H, Ar-H), 7.54-7.55 (d, *J* = 4 Hz, 4H, Ar-H), 7.46-7.44 (m, 2H, Ar-H), 7.35 (dd, *J* = 7.2, 10 Hz, 3H, Ar-H), 7.22-7.12 (m, 2H, Ar-H), 7.03-6.92 (m, 4H, Ar-H), 6.76 (d, *J* = 9.3 Hz, 2H, Ar-H), 6.61-6.40 (m, 10H, Ar-H), 1.49 (s, 18H, -CH₃).

Synthesis of **10-(4-(3,6-di-*tert*-butyl-9H-carbazol-9-yl)phenyl)-10''-(4-(4,6-diphenyl-1,3,5-triazin-2-yl)phenyl)-10H,10''H-dispiro[acridine-9,10'-indeno[2,1-b]fluorene-12',9''-acridine](*p*-D2T)**

1 (1 g, 1.05 mmol) and 2-(4-bromophenyl)-4,6-diphenyl-1,3,5-triazine (1.2g, 3.2 mmol) and toluene (20 mL) were added into a 100 mL double neck flask in N₂ atmosphere. The mixture was degassed for 10 min, acetic acid palladium (II) (80 mg, 0.36 mmol), sodium *tert*-butoxide (202 mg, 2.1 mmol), and tri-*tert*-butylphosphine tetrafluoroborate (116 mg, 0.4 mmol) were added. The mixture was heated to 110 °C and continually stirred for 8 h. After cooling and vacuum filtrating, the filtrate was evaporated under reduced pressure. Purification via column chromatography on silica gel (300-400 mesh, petroleum ether/dichloromethane = 5:1, v/v) afforded as light yellow solid (945 mg, 90% yield). ¹H NMR (400 MHz, CDCl₃) δ 9.06 (d, *J* = 8.4 Hz, 2H, Ar-H), 8.81 (d, *J* = 9.7 Hz, 4H, Ar-H), 8.33 (s, 1H, Ar-H), 8.18 (s, 2H, Ar-H), 7.94 (d, *J* = 7.5 Hz, 2H, Ar-H), 7.89 (d, *J* = 6.3 Hz, 2H, Ar-H), 7.68-7.55 (m, 12H, Ar-H), 7.54 (m, 14H, Ar-H), 7.51-7.43 (m, 2H, Ar-H), 7.38 (t, *J* = 7.8 Hz, 2H, Ar-H), 6.97 (dt, *J* = 8.6, 4.7 Hz, 2H, Ar-H), 6.92-6.85 (m, 2H, Ar-H), 6.60 (m, 9H, Ar-H), 6.47 (d, *J* = 8.4 Hz, 2H, Ar-H), 6.41 (d, *J* = 8.3 Hz, 2H, Ar-H), 1.49 (s, 18H, -CH₃). ¹³C NMR (101 MHz, CDCl₃) δ 171.89, 171.04, 158.13, 158.06, 156.01, 155.80, 145.08, 143.32, 141.66, 141.58, 141.26, 141.00, 139.29, 138.96, 138.25, 136.95, 136.84, 136.05, 132.71, 131.74, 131.60, 129.03, 128.81, 128.72, 128.41, 127.76, 127.69, 127.55, 127.32, 127.28, 125.10, 125.03, 123.80, 123.66, 120.85, 120.05, 116.39, 114.56, 114.53, 110.90, 109.25, 56.90, 34.78, 32.02. HRMS (ESI): *m/z* Calcd for C₉₁H₆₈N₆ (M+H)⁺ 1245.587, found 1245.563. Anal. Calcd. for C₉₁H₆₈N₆: C, 87.75; H, 5.50; N,

6.75. found: C, 86.52; H, 5.23; N, 6.52.

Synthesis of **10-(3-(3,6-di-tert-butyl-9H-carbazol-9-yl)phenyl)-10H,10''H-dispiro[acridine-9,10'-indeno[2,1-b]fluorene-12',9''-acridine](2)**

D2T (700 mg, 1.2 mmol) and 9-(3-bromophenyl)-3,6-di-tert-butyl-9H-carbazole (433 mg, 1 mmol) and toluene (40 mL) were added into a 100 mL double neck flask in N₂ atmosphere. The mixture was degassed for 10 min, acetic acid palladium (II) (50 mg, 0.22 mmol), sodium tert-butoxide (230 mg, 2.4 mmol), and tri-tert-butylphosphine tetrafluoroborate (100 mg, 0.345 mmol) were added. The mixture was heated to 110 °C and continually stirred for 8 h. After cooling and vacuum filtrating, the filtrate was evaporated under reduced pressure. Purification via column chromatography on silica gel (300-400 mesh, petroleum ether/dichloromethane = 2:1, v/v). White solid of **2** was obtained in 55% yield (515 mg). ¹H NMR (500 MHz, CDCl₃) δ 8.18 (d, *J*=2, 2H, Ar-H), 8.17 (s, 1H, Ar-H), 7.91-7.83 (m, 3H, Ar-H), 7.77 (d, *J* = 8.0 Hz, 1H, Ar-H), 7.64 (s, 1H, Ar-H), 7.53 (d, *J* = 10.6 Hz, 2H, Ar-H), 7.43 (d, *J* = 8.7 Hz, 2H, Ar-H), 7.41-7.26 (m, 4H, Ar-H), 7.25-7.21 (m, 2H, Ar-H), 7.14 (t, *J* = 7.5 Hz, 1H, Ar-H), 6.93 (m, *J* = 8.5, 7.0, 1.7 Hz, 2H, Ar-H), 6.88-6.81 (m, 2H, Ar-H), 6.55 (t, *J* = 7.5 Hz, 2H, Ar-H), 6.49 (dd, *J* = 7.8, 1.6 Hz, 2H, Ar-H), 6.44 (d, *J* = 7.1 Hz, 3H, Ar-H), 6.35 (d, *J* = 6.5 Hz, 2H, Ar-H), 6.28 (d, *J* = 8.0 Hz, 2H, Ar-H), 5.76 (s, 1H, Ar-H), 1.48 (s, 18H, -CH₃).

Synthesis of **10-(3-(3,6-di-tert-butyl-9H-carbazol-9-yl)phenyl)-10''-(4-(4,6-diphenyl-1,3,5-triazin-2-yl)phenyl)-10H,10''H-dispiro[acridine-9,10'-indeno[2,1-b]fluorene-12',9''-acridine] (m-D2T)**

2 (620 mg, 0.67 mmol) and 2-(4-bromophenyl)-4,6-diphenyl-1,3,5-triazine (520 mg, 1.34 mmol) and toluene (20 mL) were added into a 100 mL double neck flask in N₂ atmosphere. The mixture was degassed for 10 min, acetic acid palladium (II) (50 mg, 0.22 mmol), sodium tert-butoxide (129 mg, 1.34 mmol), and tri-tert-butylphosphine tetrafluoroborate (50 mg, 0.17 mmol) were added. The mixture was heated to 110 °C and continually stirred for 8 h. After cooling and vacuum filtrating, the filtrate was evaporated under reduced pressure. Purification via column chromatography on silica gel (300-400 mesh, petroleum ether/dichloromethane = 5:1, v/v) afforded as light yellow solid (670 mg, 84% yield). ¹H NMR (400 MHz, CDCl₃) δ 9.04 (d, *J* = 8.5 Hz,

2H, Ar-H), 8.83 (d, $J = 7.9$ Hz, 4H, Ar-H), 8.31 (s, 1H, Ar-H), 8.15 (s, 2H, Ar-H), 7.96-7.83 (m, 3H, Ar-H), 7.79 (d, $J = 8.2$ Hz, 1H, Ar-H), 7.71 (t, $J = 2$ Hz, 1H, Ar-H), 7.66-7.57 (m, 10H, Ar-H), 7.47 (m, 6H, Ar-H), 7.42-7.30 (m, 3H, Ar-H), 7.15 (t, $J = 7.4$ Hz, 1H, Ar-H), 7.01-6.92 (m, 2H, Ar-H), 6.91-6.82 (m, 2H, Ar-H), 6.59 (m, 8H, Ar-H), 6.49 (d, $J = 8.4$ Hz, 2H, Ar-H), 6.37 (d, $J = 8.0$ Hz, 2H, Ar-H), 1.47 (s, 18H, -CH₃). ¹³C NMR (101 MHz, CDCl₃) δ 171.88, 171.05, 158.18, 158.07, 155.91, 155.82, 145.08, 143.30, 142.52, 141.71, 141.64, 141.09, 140.96, 140.87, 138.80, 136.83, 136.73, 136.33, 136.08, 132.72, 132.25, 131.72, 131.59, 129.39, 129.16, 129.04, 128.74, 128.43, 127.77, 127.65, 127.53, 127.49, 127.37, 127.27, 126.39, 125.17, 125.05, 124.99, 123.93, 123.64, 120.84, 120.04, 119.99, 116.33, 114.53, 114.37, 110.84, 109.16, 56.87, 34.76, 31.99. HRMS (ESI): m/z Calcd for C₉₁H₆₈N₆ (M+H)⁺ 1245.587, found 1245.452. Anal. Calcd. for C₉₁H₆₈N₆: C, 87.75; H, 5.50; N, 6.75, found: C, 87.43; H, 5.25; N, 6.79.

Synthesis of **10-(4-(4-cyclohexyl-6-phenyl-1,3,5-triazin-2-yl)phenyl)-10''-(4-(3,6-di-tert-butyl-9H-carbazol-9-yl)phenyl)-10H,10''H-dispiro[acridine-9,10'-indeno[2,1-b]fluorene-12',9''-acridine] (c-D2T)**

1 (1.1 g, 1.2 mmol) and 2-(4-bromophenyl)-4-cyclohexyl-6-phenyl-1,3,5-triazine (435 mg, 0.94 mmol) and xylene (10 mL) were added into a 50 mL double neck flask in N₂ atmosphere. The mixture was degassed for 10 min, acetic acid palladium (II) (50 mg, 0.22 mmol), sodium tert-butoxide (181 mg, 1.88 mmol), and tri-tert-butylphosphine tetrafluoroborate (116 mg, 0.4 mmol) were added. The mixture was heated to 110 °C and continually stirred for 8 h. After cooling and vacuum filtrating, the filtrate was evaporated under reduced pressure. Purification via column chromatography on silica gel (300-400 mesh, petroleum ether/dichloromethane = 5:1, v/v) afforded as pale yellow solid (952 mg, 81% yield). ¹H NMR (400 MHz, CDCl₃) δ 8.95 (d, $J = 6.5$ Hz, 2H, Ar-H), 8.70 (d, $J = 8.0$ Hz, 2H, Ar-H), 8.33 (s, 1H, Ar-H), 8.18 (s, 2H, Ar-H), 7.93 (dd, $J = 7.6, 3.3$ Hz, 2H, Ar-H), 7.88 (d, $J = 8.5$ Hz, 2H, Ar-H), 7.67-7.53 (m, 12H, Ar-H), 7.46 (d, $J = 7.5$ Hz, 2H, Ar-H), 7.42-7.34 (m, 2H, Ar-H), 7.22 (t, $J = 8.0$ Hz, 2H, Ar-H), 6.96 (dt, $J = 8.5, 4.6$ Hz, 2H, Ar-H), 6.92-6.83 (m, 2H, Ar-H),

6.63-6.53 (m, 8H, Ar-H), 6.46 (d, $J = 8.4$ Hz, 2H, Ar-H), 6.38 (d, $J = 8.4$ Hz, 2H, Ar-H), 2.97 (t, $J = 11.5$ Hz, 1H, -CH₃), 2.17 (d, $J = 12.1$ Hz, 2H, -CH₃), 1.96-1.75 (m, 5H, -CH₃), 1.49 (s, 18H, -CH₃), 1.39-1.22 (m, 3H, -CH₃). ¹³C NMR (101 MHz, CDCl₃) δ 183.30, 171.44, 170.59, 158.18, 158.14, 156.06, 155.84, 144.90, 143.36, 141.72, 141.61, 141.29, 141.04, 139.33, 139.00, 138.29, 136.98, 136.84, 136.50, 136.16, 132.74, 132.54, 131.70, 131.57, 128.97, 128.85, 128.70, 128.45, 127.80, 127.72, 127.58, 127.36, 127.30, 125.13, 125.10, 125.02, 123.84, 123.71, 120.87, 120.09, 116.43, 114.58, 110.94, 109.30, 56.93, 47.19, 34.82, 32.06, 31.29, 26.08, 26.05. HRMS (ESI): m/z Calcd for C₉₁H₇₄N₆ (M+H)⁺ 1250.597, found 1250.287. Anal. Calcd. for C₉₁H₇₄N₆: C, 87.73; H, 5.96; N, 6.71, found: C, 87.30; H, 5.75; N, 6.58.

Exciton Lifetime and Rate Constant

The rate constants of ISC (k_{ISC}) and RISC (k_{RISC}) of three emitters based on the following equations:

$$k_p = \frac{1}{\tau_p} \quad (1)$$

$$k_d = \frac{1}{\tau_d} \quad (2)$$

$$k_{r,s} = \Phi_p k_p + \Phi_d k_d \approx \Phi_p k_p \quad (3)$$

$$k_{RISC} \approx \frac{k_p k_d \Phi_d}{k_{r,s}} \quad (4)$$

$$k_{ISC} \approx \frac{k_p k_d \Phi_p}{k_{RISC} \Phi_d} \quad (5)$$

In this study, the prompt PLQY (Φ_p) and delayed PLQY (Φ_d) were determined by using the total PLQY and the integrated intensity ratio between prompt and delayed components which was calculated from transient photoluminescence measurements.

The intensity ratio between prompt (r_p) and delayed (r_d) components were determined

using two fluorescent lifetimes (τ_p , τ_d) and fitting parameter (A_p , A_d) as follow.

$$I(t) = A_p e^{-\frac{t}{\tau_p}} + A_d e^{-\frac{t}{\tau_d}} \quad (6)$$

$$r_p = \frac{A_p \tau_p}{A_p \tau_p + A_d \tau_d} \quad (7)$$

$$r_d = \frac{A_d \tau_d}{A_p \tau_p + A_d \tau_d} \quad (8)$$

Then, the prompt PLQY (Φ_p) and delayed PLQY (Φ_d) were determined using intensity ratio (r_p , r_d) and total PLQY.

$$\Phi_{total} = \Phi_p + \Phi_d \quad (9)$$

$$\Phi_p = r_p \Phi_{total} \quad (10)$$

$$\Phi_d = r_d \Phi_{total} \quad (11)$$

Supplementary Figures and Tables

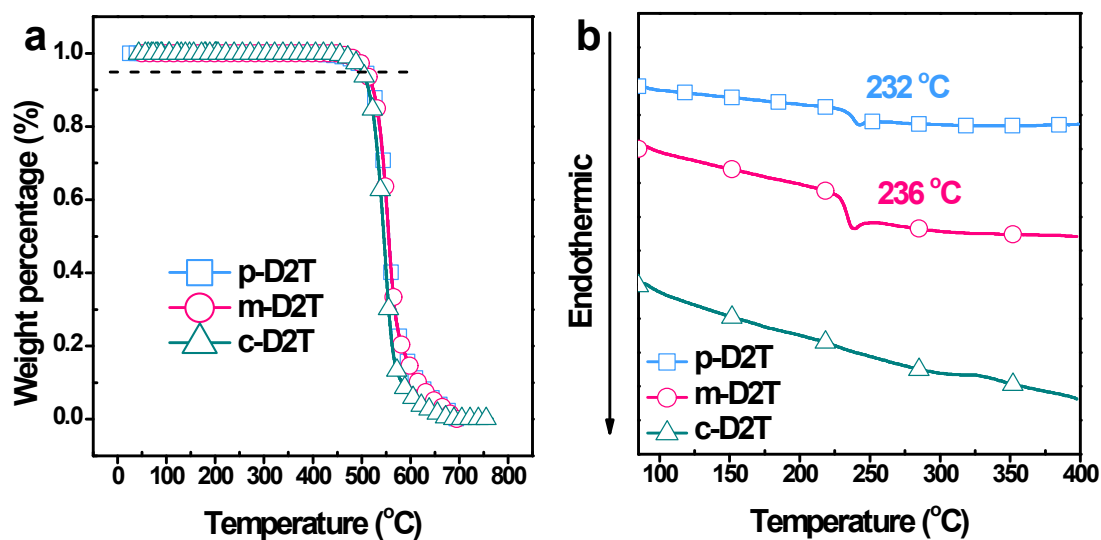


Figure S1. (a) TGA and (b) DSC curve of **p-D2T**, **m-D2T** and **c-D2T** under the heating rate of 10 K/min under N_2 .

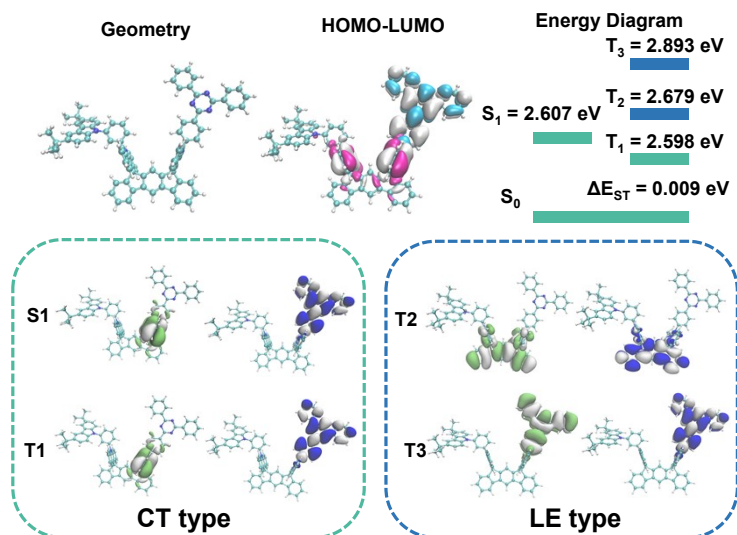


Figure S2. Theoretical simulation results of ground and excited states of **m-D2T** using DFT under B3LYP/6-31g** level and TD-DFT under pbe0/def2SVP level, respectively. Cyan, magenta, lime and blue: distribution of LUMO, HOMO, hole NTO and particle NTO.

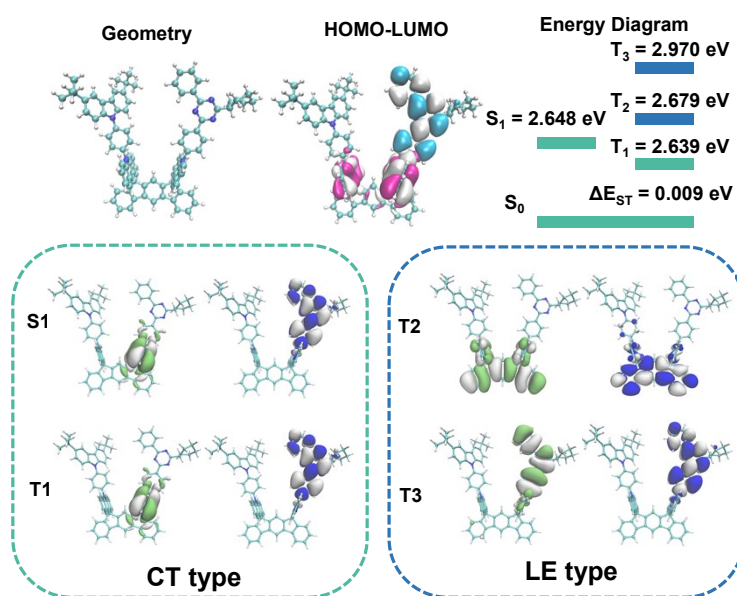


Figure S3. Theoretical simulation results of ground and excited states of **c-D2T** using DFT under B3LYP/6-31g** level and TD-DFT under pbe0/def2SVP level, respectively. Cyan, magenta, lime and blue: distribution of LUMO, HOMO, hole NTO and particle NTO.

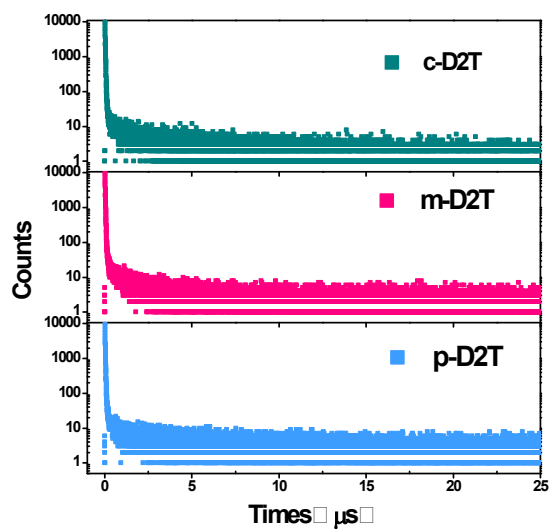


Figure S4. Transient PL decay of **p-D2T**, **m-D2T** and **c-D2T** in doped films (10 wt% in DPEPO) under oxygen free atmosphere in the scale of 25 μ s.

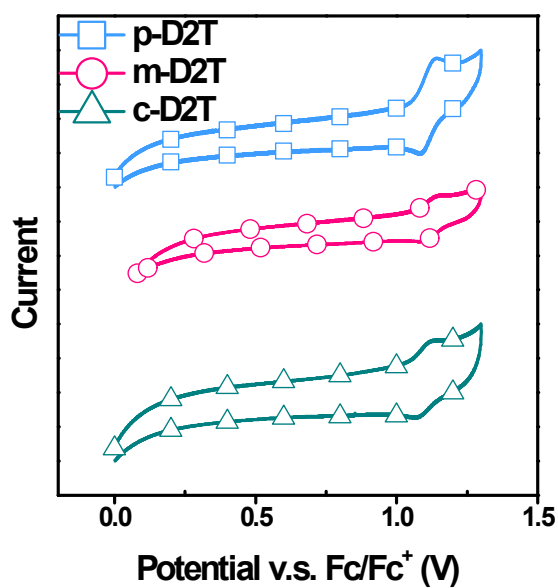


Figure S5. CV profiles of cyclic voltammetry analysis of **p-D2T**, **m-D2T** and **c-D2T** at a scan rate of 100 mV/s

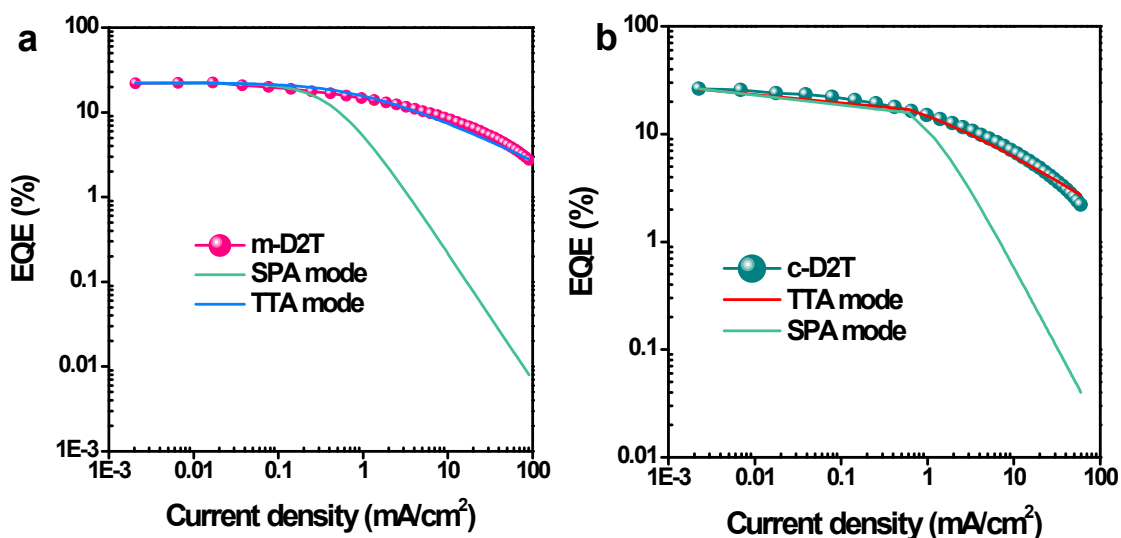


Figure S6. The EQE- J curves and the fitting lines of TTA and SPA for a) **m-D2T** and b) **c-D2T**.

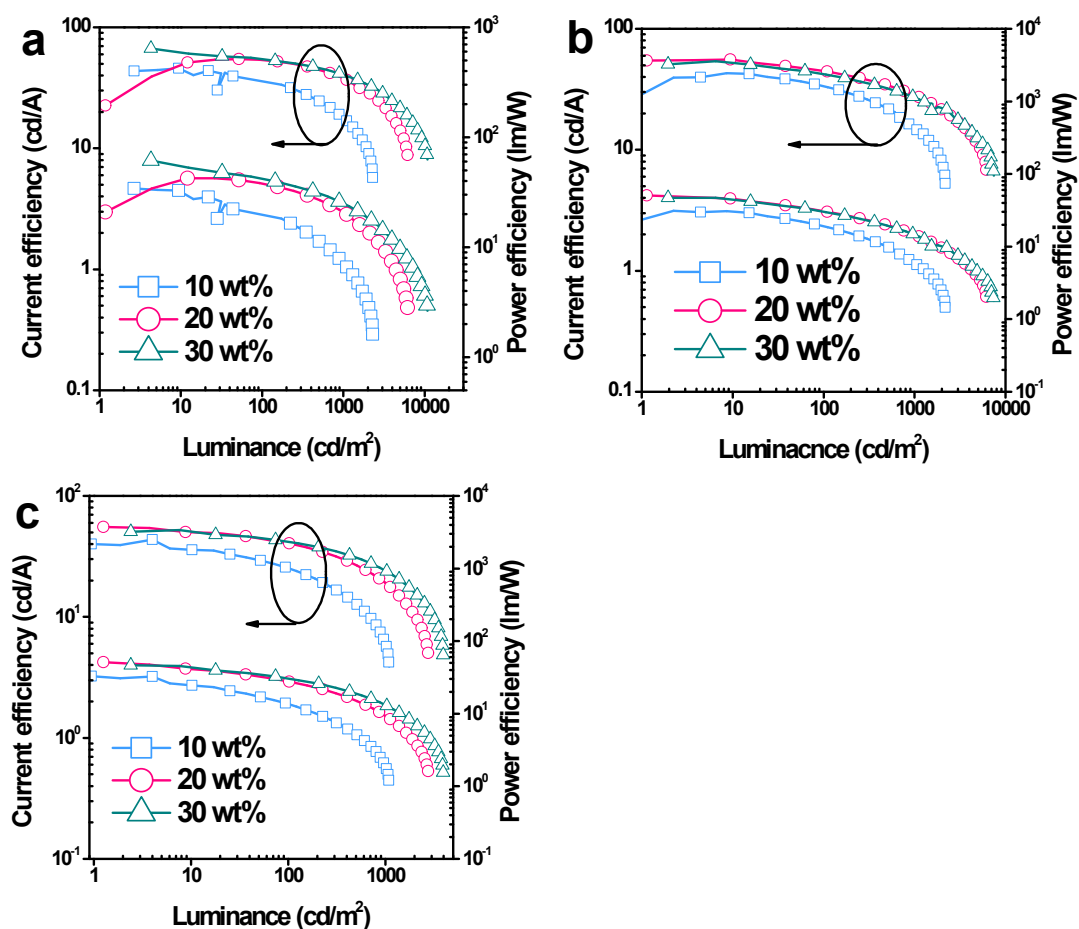


Figure S7. Current efficiency and power efficiency versus Luminance profiles of devices based on **p-D2T**, **m-D2T** and **c-D2T** under various doping concentrations.

Table S1. Crystallographic data for p-D2T.

Compound	p-D2T
CCDC No.	2128754
Formular	C ₉₁ H ₆₈ N ₆
Formula weight	1245.51
Crystal system	monoclinic
Space group	P21/n
a/Å	18.7905(19)
b/Å	18.7820(18)
c/Å	21.137(2)
α /°	90
β /°	113.331(3)
γ /°	90
Volume/Å ³	6849.8(12)
Z	4
$\rho_{\text{calc}}/\text{cm}^3$	1.208
μ/mm^{-1}	0.070
F(000)	2624.0
Crystal size/mm ³	0.15 × 0.08 × 0.05
2 Θ range (deg)	4.198 to 51.384
Goodness-of-fit on F ²	1.027
R ₁ /wR ₂ [$I \geq 2\sigma(I)$]	0.0555/0.1237

Table S2. Data of SOC matrix of p-D2T, m-D2T and m-D2T.

	SOC _{S1-T1} (cm ⁻¹)	SOC _{S1-T2} (cm ⁻¹)	SOC _{S1-T3} (cm ⁻¹)
p-D2T	0.01789	0.02299	0.70354
m-D2T	0.01435	0.03262	0.71105
c-D2T	0.06550	0.20198	0.72130

Reference

1. T. Lu, F. Chen, F., Multiwfn: a multifunctional wavefunction analyzer. *J Comput*

Chem **2012**, *33*, 580-592.

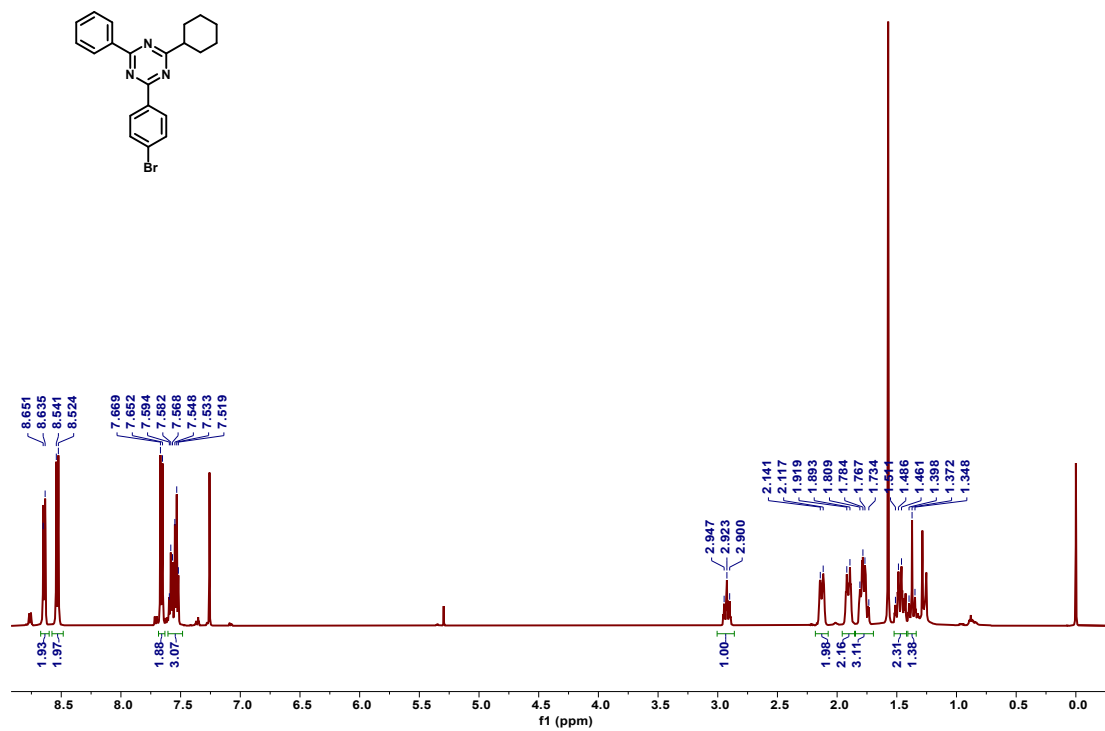
2. W. Sun, N.L. Zhou, Y. Xiao, S.R. Wang, X.G. Li, Novel carbazolyl-substituted spiro[acridine-9,9'-fluorene] derivatives as deep-blue emitting materials for OLED applications. *Dyes Pigm.* **2018**, *154*, 30-37.

3. J. Hu, Q. Li, X.D. Wang, S.Y. Shao, L.X. Wang, X.B. Jing, F.S. Wang. Developing through-space charge transfer polymers as a general approach to realize full-color and white emission with thermally activated delayed fluorescence. *Angew. Chem. Int. Ed.* **2019**, *58*, 8405-8409.

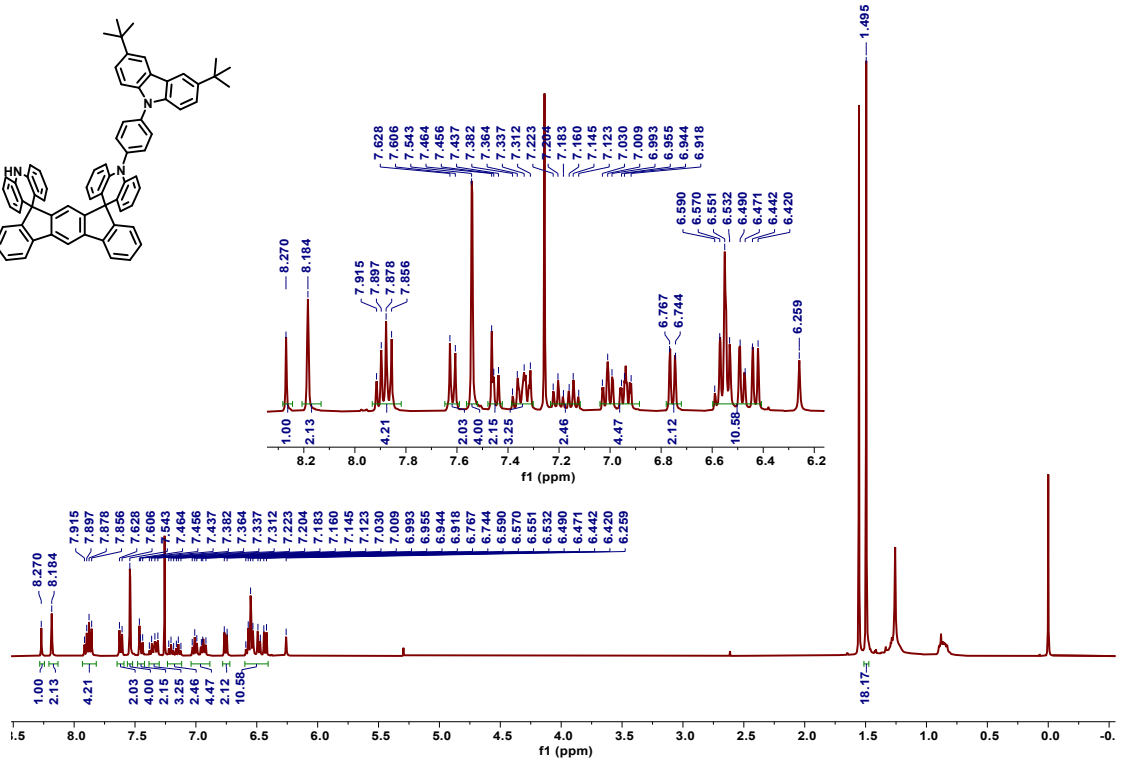
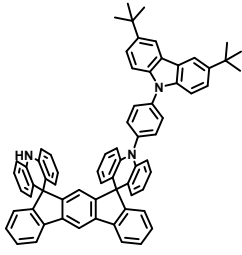
4. Z.W. Liu, G.G. Li, H. Liu, C.J. Zhou, K. Li, Z.M. Wang, C.L. Yang, Side by Side Alignment of Donors Enabling High-Efficiency TADF OLEDs with Insensitivity to Doping Concentration. *Adv. Optical. Mater.* **2021**, *9*, 2101410

NMR spectra

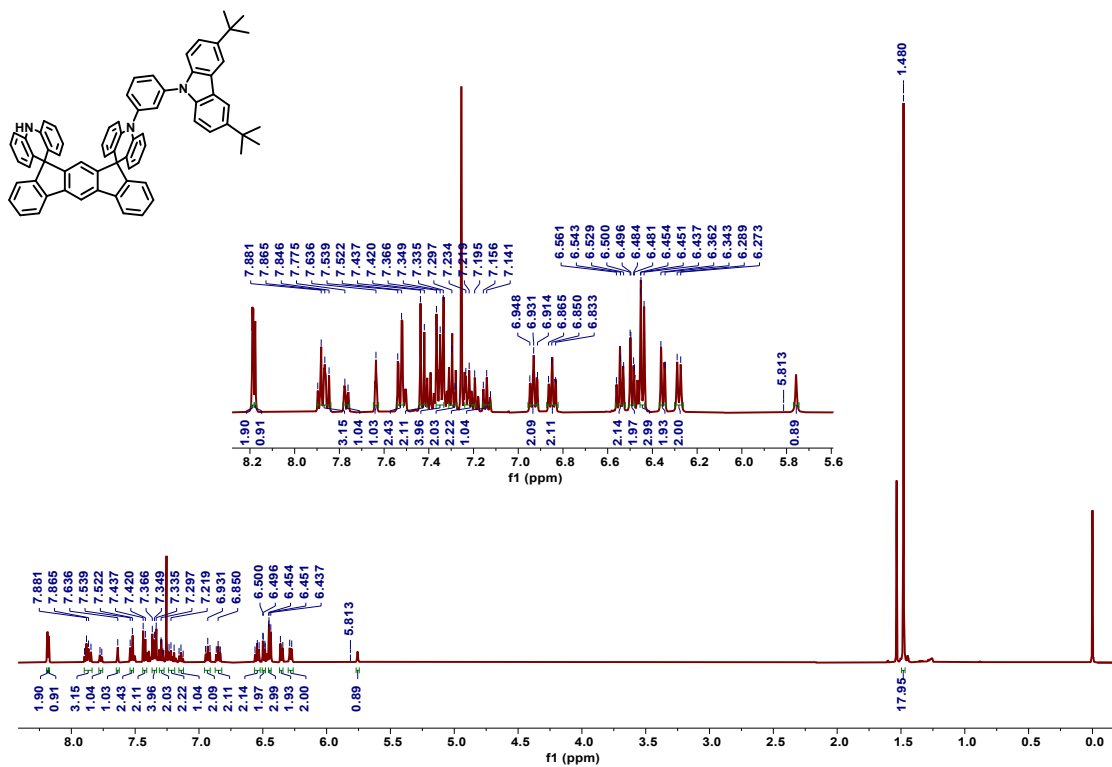
^1H NMR spectra of *2-Chloro-4-cyclohexyl-6-phenyl-1,3,5-triazine* (CDCl_3)



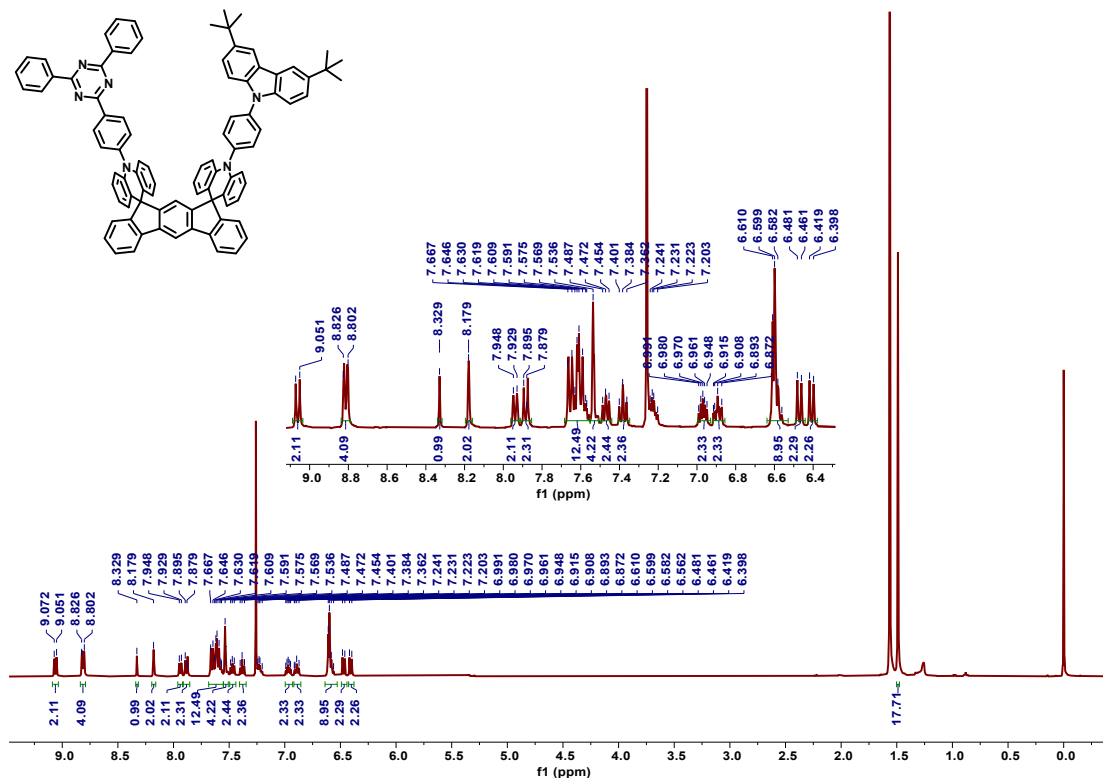
^1H NMR spectra of **1** (CDCl_3)



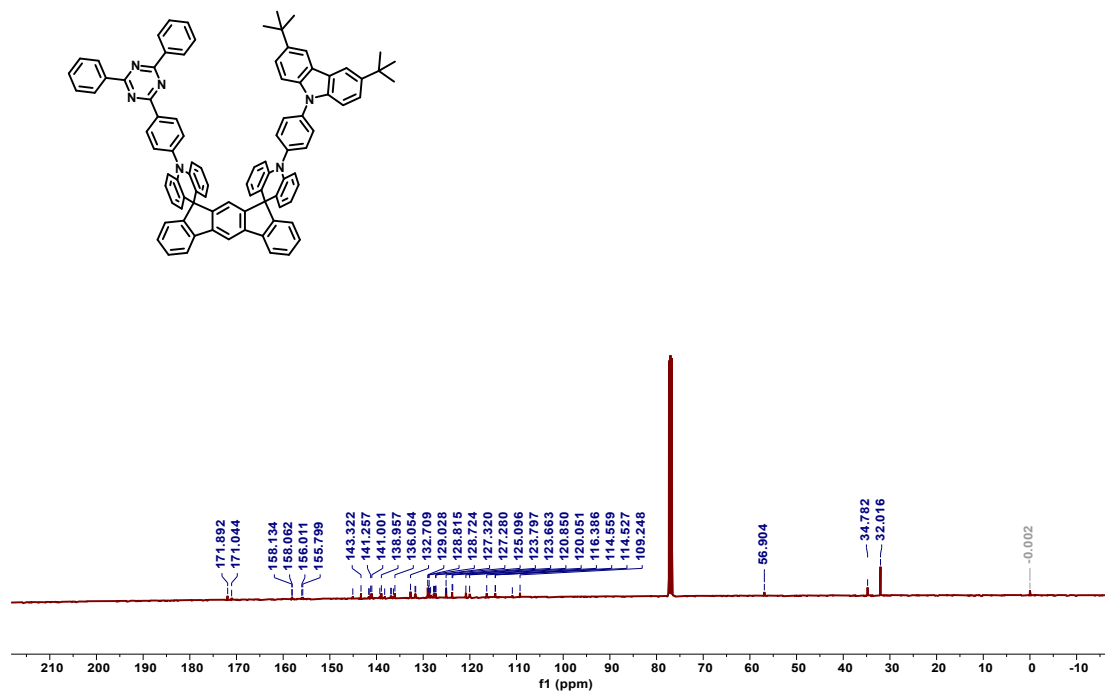
¹H NMR spectra of **2** (CDCl₃)



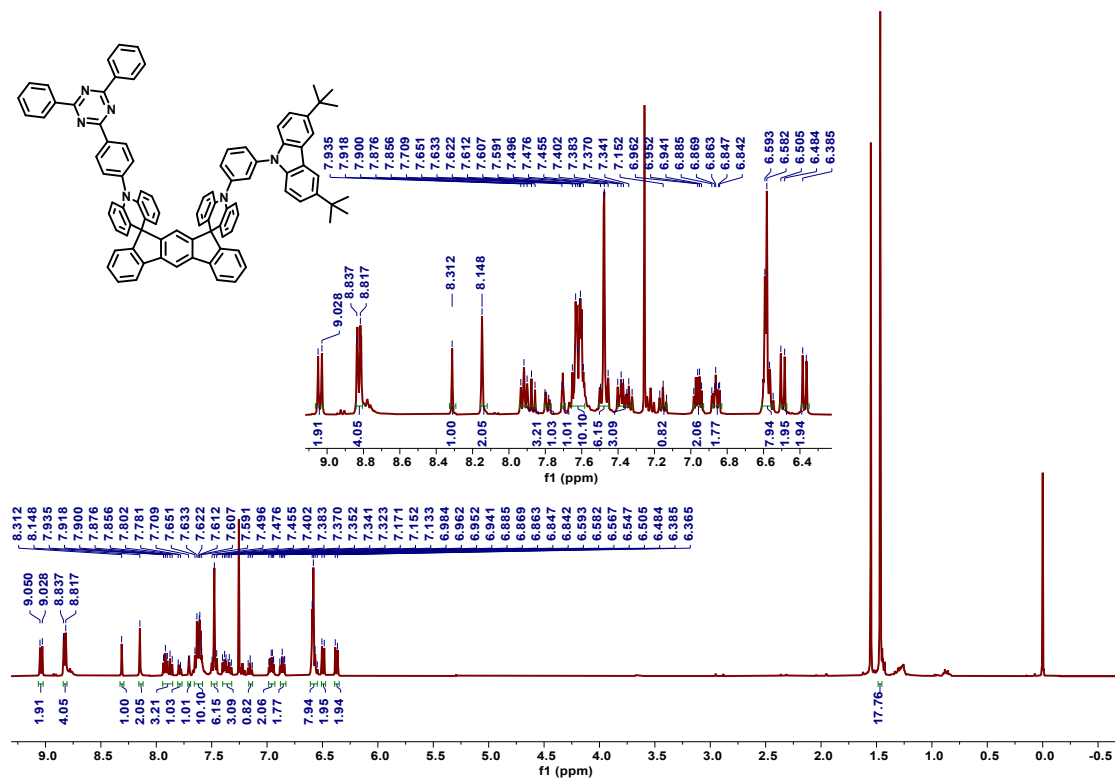
¹H NMR spectra of **p-D2T** (CDCl₃)



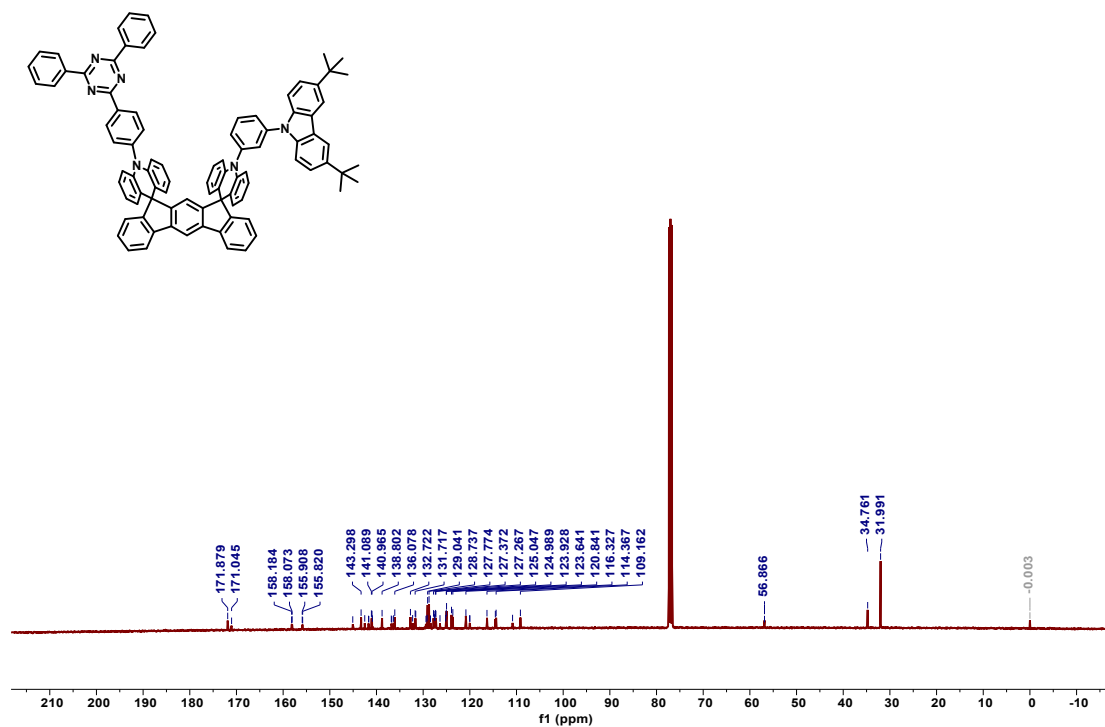
¹³C NMR spectra of **p-D2T** (CDCl₃)



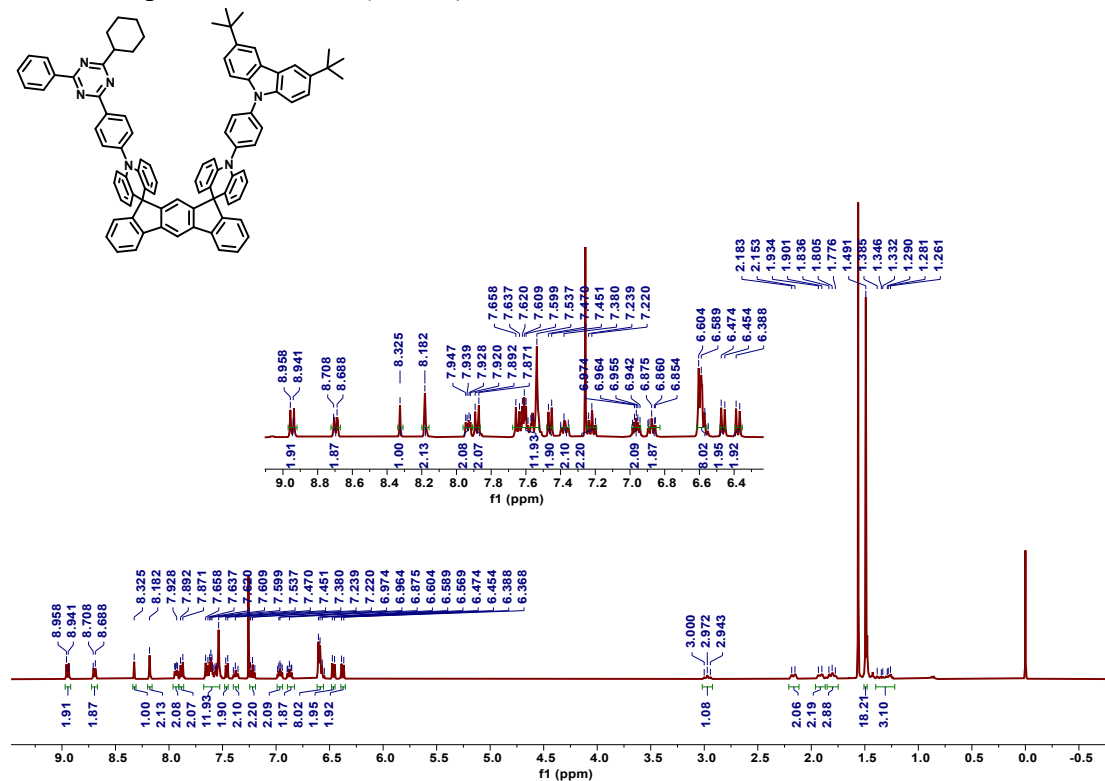
¹H NMR spectra of **m-D2T** (CDCl₃)



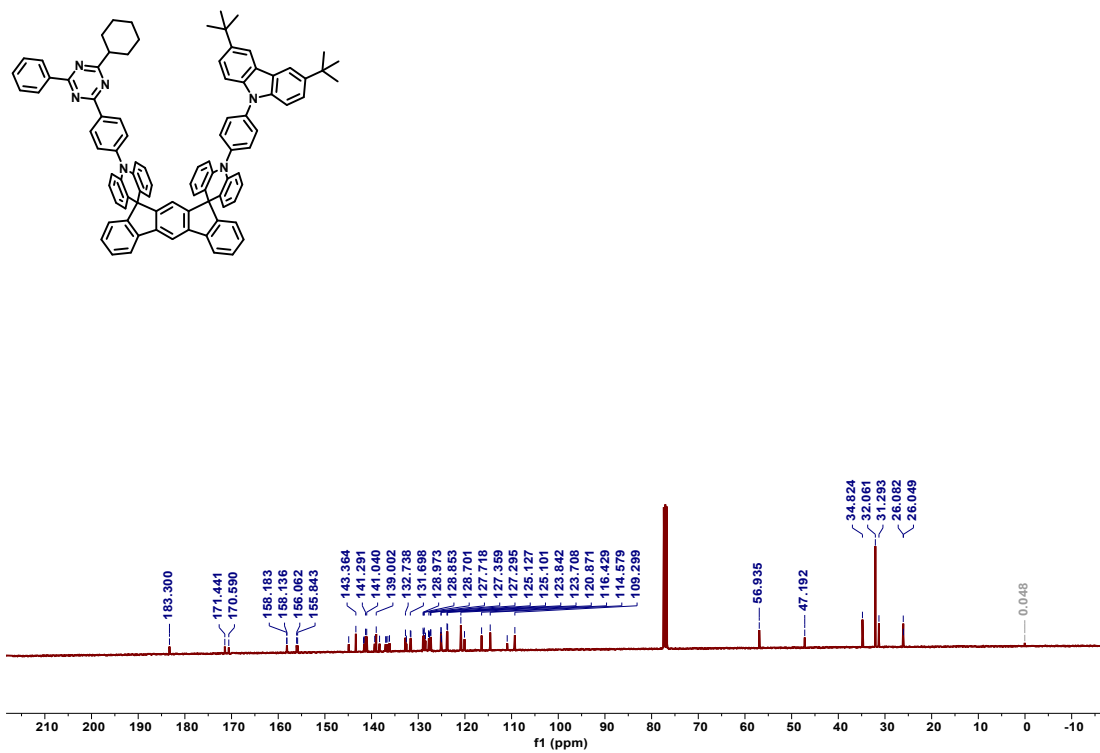
^{13}C NMR spectra of **m-D2T** (CDCl_3)



^1H NMR spectra of **c-D2T** (CDCl_3)

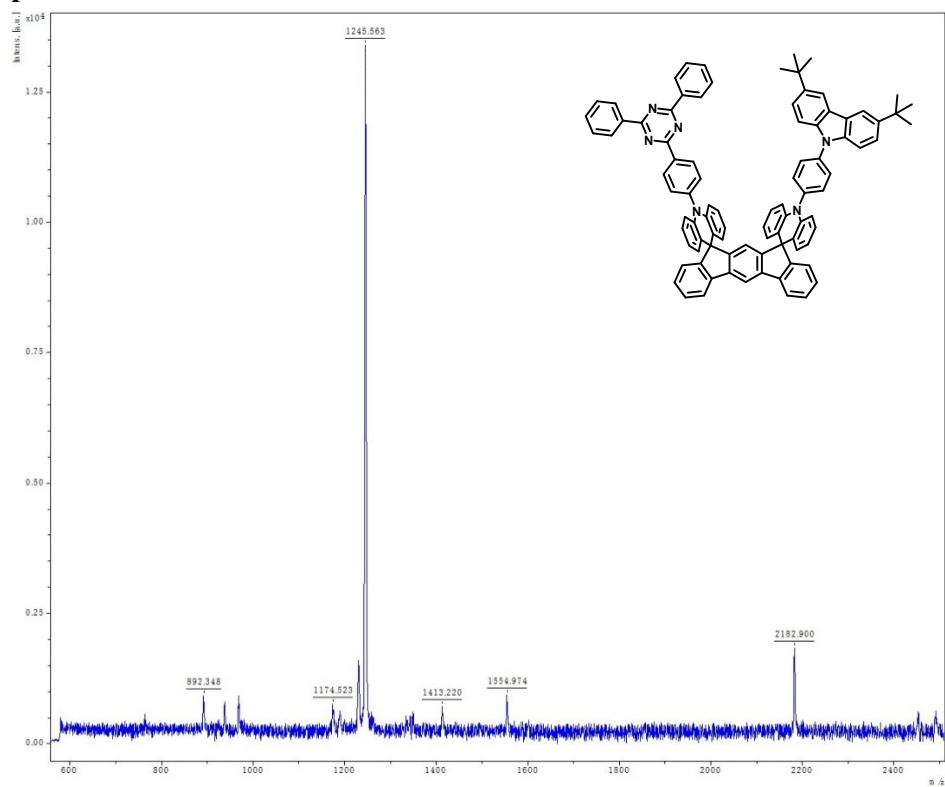


^{13}C NMR spectra of **c-D2T** (CDCl_3)

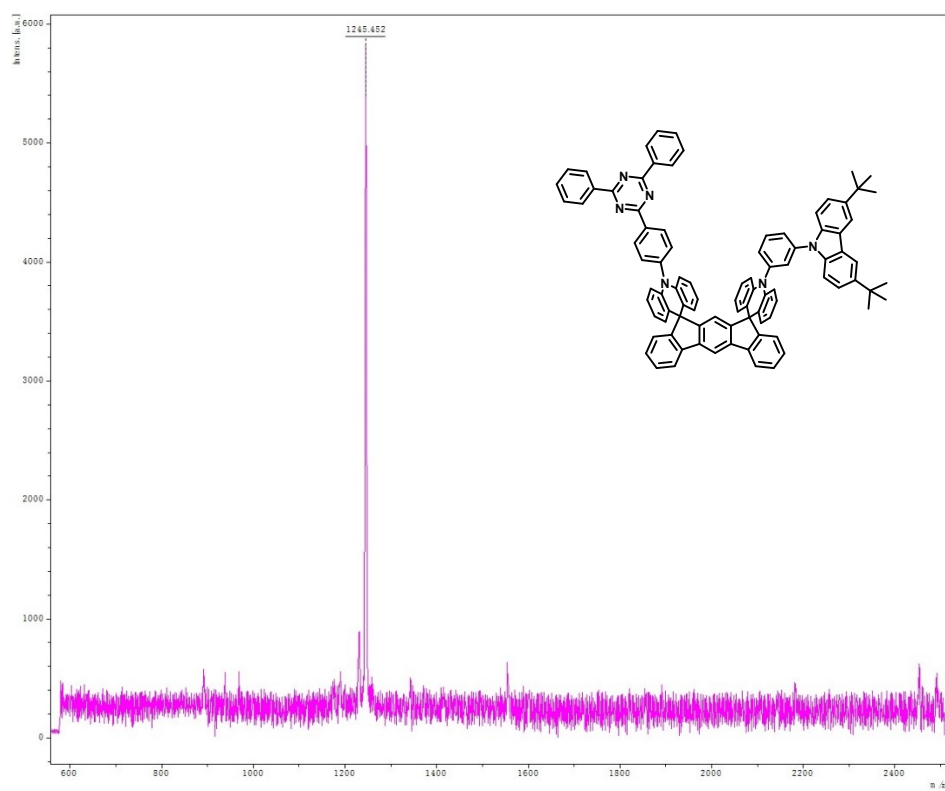


Mass spectrometry

p-D2T



m-D2T



c-D2T

